Pergamon

Int. J. Mach. Tools Manufact. Vol. 37, No. 9, pp. 1201–1217, 1997

Printed in Great Britain
0890-6955/97$17.00 + .00

PII: S0890-6955(97)00013-8

ON-LINE PREDICTION OF SURFACE FINISH AND DIMENSIONAL DEVIATION IN TURNING USING NEURAL NETWORK BASED SENSOR FUSION

R. AZOUZI† and M. GUILLOT‡

(*Received* 15 *September* 1995; *in final form* 1 *December* 1996)

Abstract—This paper examines the feasibility for an intelligent sensor fusion technique to estimate on-line surface finish (*Ra*) and dimensional deviations (*DD*) during machining. It first presents a systematic method for sensor selection and fusion using neural networks. Specifically, the turning of free-machining and low carbon steel is considered. The relationships of the readily sensed variables in machining to *Ra* and *DD*, and their sensitivity to process conditions are established. Based on this experimental data and using statistical tools, the sensor selection and fusion method assists the experimenter in determining the average effect of each candidate sensor on the performance of the measuring system. In the case studied, it appeared that the cutting feed, depth of cut and two components of the cutting force (the feed and radial force components) provided the best combination to build a fusion model for on-line estimation of *Ra* and *DD* in turning. Surface finish was assessed with an error varying from 2 to 25% under different process conditions, while errors ranging between 2 and 20 μm were observed for the prediction of dimensional deviations. © 1997 Published by Elsevier Science Ltd. All rights reserved

1. INTRODUCTION

Today more than ever, manufacturing calls for better product quality at a lower cost. For instance in machining, the quality of machined parts plays a crucial role in the functional capacity of the part and, therefore, a great deal of attention should be paid to keep consistent tolerances and surface finish.

Typically, three phenomena are at the origin of a poor surface finish on parts issued from machining: (i) the tool geometry and kinematics relative to the part often called feed marks; (ii) self-excited and machine tool vibrations; and finally (iii) surface plastic deformation resulting from a worn tool, built-up edge or material softening that occur especially at high temperature and insufficient cooling. On the other hand, accuracy is highly affected by the cutting forces and the stiffness of the cutting tool, the tool holder and part fixtures. Even with very stiff and accurate machine tools and lower values of parameters such as cutting feed, speed and depth of cut, several constraints still limit the improvement of part dimensional accuracy and surface finish [1]. Among them are the progressive wear and deflection of the cutting tool, the variation of process conditions during the cutting operation, etc. (see Fig. 1).

Adaptive control has been viewed as a promising strategy to adapt on-line the process parameters to the widely varying machining conditions. In fact, a great deal of research in machining has been dedicated to on-line control of surface finish and dimensional accuracy [2–4]. So far, no such adaptive systems have been implemented in industry—the most important reasons being: (i) the absence of rugged sensing devices that provide part quality measurements reliably and effectively in an hostile machining environment; and (ii) the lack of in-depth understanding of the cutting process leading to inadequate models [5–7].

Sensor development for quality characteristics measurements such as on-line surface finish and dimensional deviation (*Ra* and *DD*) has followed two major trends: direct and indirect methods.

†Mechanical Engineering Department, Laval University, Quebec, Canada G1K 7P4
‡†To whom correspondence should be addressed.

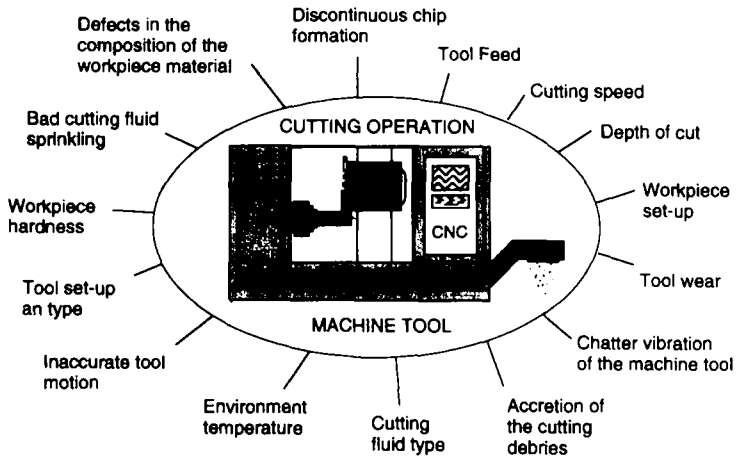

Fig. 1. Factors affecting part quality.

As shown in Fig. 2(a), direct sensing methods measure the quality characteristics directly from the workpiece. However, direct *DD* and *Ra* sensors were not usually successful in producing reliable on-line measurements [8]. Contacting sensors (e.g. sensors using a stylus) are often ineffective mainly due to wear, fracture, vibration and chip evacuation problems, while noncontacting sensors (e.g. interferometry or capacitance-based sensors) are impractical mainly due to the interference of chips and cutting fluid. On the other hand, in indirect sensing the sensor measures physical quantities such as cutting vibrations and forces [see Fig. 2(b)]. The output signal is fed into a mathematical model which estimates the value of the investigated characteristics. For example, in Ref. [9], El-Karamany used cutting force measurements to estimate the *DD* on slender turned workpieces. The model includes many compliance-related machining parameters which are difficult to determine in practice. In Ref. [4], Watanabe and Iwai estimated the surface waves and locational errors in milling from the measurements of bending moments generated in the tool holder by the cutting force. Luk *et al.* [10] utilized a vision system to assess surface finish. Using a fast Fourier transform algorithm, the captured image is transformed into a spatial frequency record which is then correlated to surface finish using a least-squares regression technique. In general, these methods are still under development and face the same problems as direct methods.

Recently, more attention has been directed at using and improving sensor fusion techniques [12]. As depicted in Fig. 2(c), the fusion of sensors is basically an indirect method. A combination of sensor signals are input into the fusion model, which is basically a mathematical function developed to extract corroborative and relevant information on the state of the manufacturing operation. In machining, sensor fusion is motivated from a

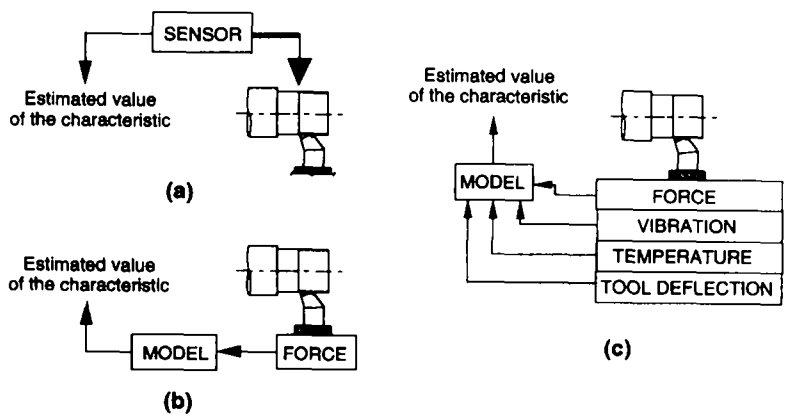

Fig. 2. Sensing methods: (a) direct method; (b) indirect methods; (c) fusion method.

viewpoint where only a few sensors can be applied and each sensor measures a different variable. Thus, by analogy with a human operator using his own physical senses to extract meaningful information on the state of the cutting operation, a sensor fusion system can be established to estimate *Ra* and *DD*. The system may use only basic sensors which operate reliably in an industrial environment [see Fig. 2(c)].

Two major difficulties are encountered when applying the fusion of sensors. These are the adequate selection of input sensors, and the establishment of an effective fusion model. It is important to ensure that all selected sensors provide relevant data correlated to the state of the manufacturing process being investigated. Obviously, it is hard to imagine that sensors meeting these specifications can have a linear output with respect to the sensed features.

Research in sensor fusion has a relatively short history in machining. Thus, no systematic and efficient method for sensor selection can be found in the machining literature. In fact, sensor fusion has been very often associated only with the problem of establishing the relationship between the sensed variables and the investigated features. Two broad categories of models can be defined: (i) theoretical, and (ii) empirical.

Theoretical models are often very difficult to develop because of the poor understanding of fundamental behavior of machining processes. For instance, Table 1 summarizes the qualitative relationships between surface finish, the size of the machined part, and the basic sensing techniques in machining as established by Birla [8]. Very often these relationships are either not understood or simply unknown. On the other hand, as shown previously, most existing theoretical models are limited to very few measurable variables and sensors, thus leaving no choice but to use empirical modeling methods. Empirical modeling methods utilize experimental data to tune the parameters of the model. In return, they compensate for the inability to completely understand and adequately describe the process mechanisms.

Typically, sensors are chosen based on available knowledge of the relationship between the sensor measurements and the feature. As recommended by Rangwala and Dornfeld [13], easily available information on the operation of the process can also be used to establish the fusion model. The latter can be implemented using a multivariate technique such as multiple regression, the group method of data handling (GMDH) or neural networks.

Chryssolouris and Guillot [14] showed that models built from neural networks were in general superior to conventional modeling techniques such as polynomial fits using multiple regression or GNDH. In fact, neural networks offer unexpected possibilities for continuous modeling. When properly trained, they are able to accurately represent process states within the range in which they have been trained despite the presence of complex interrelated phenomena occurring during processing [15]. They are trained by supervision; input–output exemplars are presented to the network which adapts its learning parameters using a training algorithm. According to Simpson [16], neural networks are very advantageous in situations where nonlinear mappings must be automatically acquired from the training data.

In this paper, a new sensor selection and fusion method is proposed and implemented to develop a sensor fusion system intended for the prediction of part surface finish and dimensional deviations during machining. In order to select sensors, this method combines

Table 1. Qualitative relationships between quality and readily sensed variables in machining

	Tool force	Cutting torque	Cutting power	Remote vibratory motion	Sound	Cutting temperature	Tool nose line
DD	—	—	—	—	—	—	Fair
Ra	Fair	—	—	Poor	?	—	—

— Denotes insignificant or "none".
? Denotes unknown.

the neural network modeling technique and statistical tools in a scheme which takes advantage of an efficient test strategy. Then, the final fusion model is built by training a neural network. The availability of experimental data exemplars obtained under a variety of machining parameters and conditions is crucial to a successful implementation of the proposed sensor selection and fusion method. Accordingly, the procedure of collecting experimental data obtained in single point turning of SAE-1018 steel under a variety of machining conditions, will be presented in detail. The collected experimental data will be first used to evaluate statistically the traditional indirect sensing techniques used in machining, including cutting forces, vibration, acoustic emission and tool deflections.

2. EXPERIMENTAL CHARACTERIZATION OF *RA* AND *DD* AND ANALYSIS OF SENSOR RESPONSES

Numerous factors influence the surface finish during turning operations. Accordingly, as shown in the cause–effect diagram of Fig. 3, this study will be restricted to only seven of them. The first three factors are the cutting parameters which include the cutting feed, speed and depth of cut (f, v and d, respectively). The four other factors include the process conditions that are believed to influence significantly quality in machining [1, 8]. These are the cutting fluid flow, the tool wear state, the workpiece diameter to simulate the stiffness of the tool fixturing system, and the part-to-part variation of work material properties (F, W, D and P, respectively). The effects of all the latter factors on the readily sensed variables in machining including the three components of the cutting forces (F_s, F_r and F_z), tool–workpiece system vibration (Vb), acoustic emissions (AE), and tool deflections along the speed and feed directions (D_s and D_z, respectively) will also be analyzed.

2.1. *Experimentation and data analysis tools*

2.1.1. *Experiments planning.* When designing experiments, very often experimenters resort to approaches such as the evaluation of the effects of one factor at a time or to a factorial design [17]. The latter design would obviously lead to a large number of tests. In contrast, the use of an efficient testing strategy such as the orthogonal arrays (OAs) developed by Taguchi [19] would minimize this number of tests. In addition, an advantage of an OA design is its equal representation of all factors; some combinations of factors and factor levels are tested which otherwise would have not been investigated. Accordingly, the OAs will be used here for the design of experiment and models.

As shown in Fig. 3, parameters f, v and d were assigned four different levels varying from 0.1 to 0.4 mm/rev, 180 to 300 m/min and 0.5 to 3.5 mm, respectively. These ranges

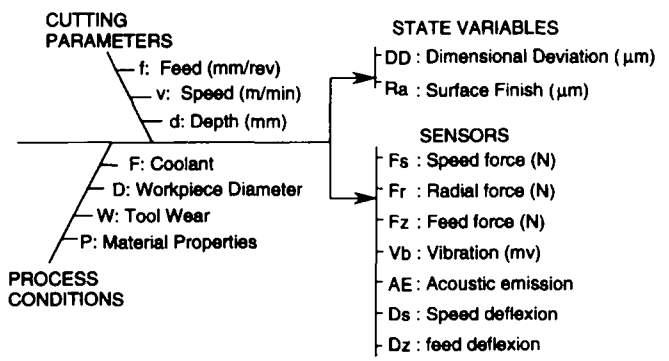

Cutting Feed (mm/rev)	Cutting speed (m/min)	Depth of cut (mm)
f1 = 0.1	v1 = 180	d1 = 0.5
f2 = 0.2	v2 = 220	d2 = 1.5
f3 = 0.3	v3 = 260	d3 = 2.5
f4 = 0.4	v4 = 300	d4 = 3.5

Cutting fluid	Part diameter	Tool wear	Material properties
F1: Good flow	D1: 100 mm	W1: Fresh tool	P1: Normal
F2: Bad flow	D2: 60 mm	W2: 0.3 mm worn	P2: Modified

Fig. 3. Turning process cause–effect diagram and factor levels.

are recommended by the manufacturer of the cutting tool for general purpose and finish turning operations of free-machining and low carbon steels. On the other hand, the cutting conditions were fixed to two levels only. Inadequate application of cutting fluid was simulated by reducing its flow rate and changing slightly its orientation. A tool was considered to be worn when its flank land reached 0.25 mm. Finally, to intentionally induce variation in part material properties, a stress relief at 600°C was practiced on the workpiece. As shown in Table 2, the orthogonal array that best fits this experiment is the L_{16} [19] with a total of 16 tests. In order to test the repeatability of the sensors and eventually evaluate the capacity of our fusion model, another set of five tests were designed as shown in Table 3. These tests are repeated six times.

2.1.2. *Experimentation.* The tests have been carried out on a Mori Seiki 25SL/MC 20HP turning center equipped with a Fanuc 15TF control system. A Kennametal CNMP-32 turning cutter with grade KC920 inserts and Sunoco Sunicut 151 cutting fluid for temperature control and chip evacuation were used for single-point turning operations on AISI-1018 steel. As illustrated in Fig. 4, the cutting tool was fixed on a piezoelectric dynamometer bolted rigidly on the tool turret so that the speed, normal and feed components of the cutting forces could be measured. An accelerometer, an acoustic emission transducer and two capacitance probes mounted close to the tool holder measured, respectively, the radial acceleration due to the workpiece–cutting tool system vibrations, the acoustic waves generated by the machining operation, and the tool deflections in the feed and speed directions.

All sensor signals were acquired at a frequency of 880 Hz and then conditioned so that only the steady-state portions were kept and averaged as shown in the example of Fig. 5. For a machined part, the *DD* is simply the difference between the reference and finished part diameters. These diameters are measured using an accurate micrometer. On the other hand, the *Ra* had been measured after the cutting operations using a portable Mitutoyo

Table 2. Training exemplars: design of experiments

Cutting parameters				Process conditions		
f (mm/rev)	v (m/min)	d (mm)	F	D	W	P
0.1	180	0.5	F1	D1	W1	P1
0.4	300	3.5	F1	D1	W1	P1
0.2	220	3.5	F1	D1	W3	P3
0.3	260	0.5	F1	D1	W3	P3
0.1	260	3.5	F3	D3	W1	P3
0.4	220	0.5	F3	D3	W1	P3
0.2	300	0.5	F3	D3	W3	P1
0.3	180	3.5	F3	D3	W3	P1
0.3	300	1.5	F1	D3	W1	P3
0.2	180	2.5	F1	D3	W1	P3
0.4	260	2.5	F1	D3	W3	P1
0.1	220	1.5	F1	D3	W3	P1
0.3	220	2.5	F3	D1	W1	P1
0.2	260	1.5	F3	D1	W1	P1
0.4	180	1.5	F3	D1	W3	P3
0.1	300	2.5	F3	D1	W3	P3

Table 3. Checking exemplars: design of experiments

Cutting parameters				Process conditions		
f (mm/rev)	v (m/min)	d (mm)	F	D	W	P
0.125	240	0.75	F2	D2	W2	P2
0.350	290	0.75	F2	D2	W2	P2
0.125	290	2.00	F2	D2	W2	P2
0.200	320	1.00	F2	D2	W2	P2
0.050	200	1.00	F2	D2	W2	P2

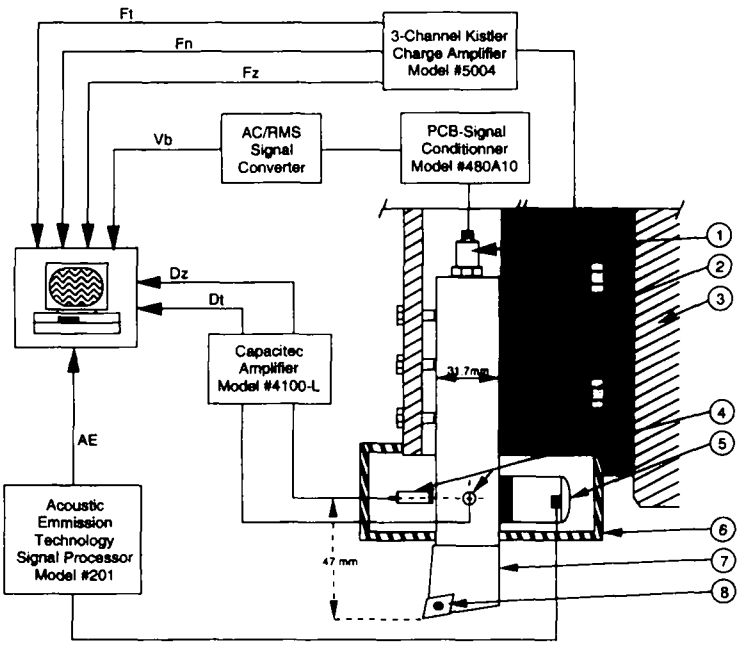

1- PCB Accelerometer, Model #353M77
2- Kistler 3-Components Piezoelectric Dynamometer, Type 9265B
3- Lathe Turret
4- Capacitec Probes, Model #HPT-40
5- Acoustic Emission Technology Transducer
6- Plastic protection shell
7- Kennametal Tool-holder, Model #CNMP32
8- Cutting inserts,Grade KC910

Fig. 4. Experimental set-up.

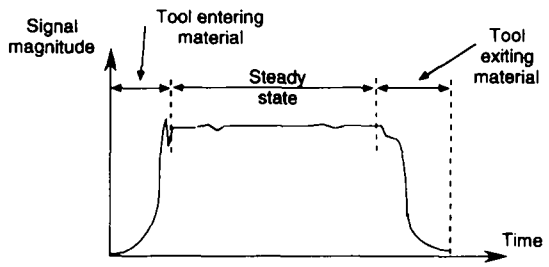

Fig. 5. Signal conditioning.

Surftest profilometer with a roughness cut-off of 0.8 mm. The results of the first set of tests are reported in Tables 2 and 4, while only the results of the 5th repetition of the second set of tests are presented in Tables 3 and 5.

2.1.3. *Data analysis tools.* The experimental data was analyzed using the following statistical tools: (i) the percent contribution from an analysis of variance, (ii) the average effect of every factor level, and (iii) the correlation between sensor measurements and the characteristics *Ra* and *DD*. The percent contribution of a factor F, denoted P_F, reflects the portion of the total variation observed in an experiment attributed to this factor [19]. Ideally, the total percent contribution of all considered factors must add up to 100. If not, the difference is the contribution of some other uncontrolled factors and experimental errors. P_F is given by Eqn (1) where SS_F is the sum of squares due to factor F and SS_T the total sum of squares:

$$P_F = \frac{SS_F - V_e \nu_F}{SS_T} 100 \tag{1}$$

Table 4. Training exemplars: sensors measurements, and *DD* and *Ra*

F_x (N)	F_r (N)	F_z (N)	*Vb* (mv)	*AE* (mv)	D_z (μm)	D_x (μm)	*DD* (μm)	*Ra* (μm)
− 143	96	69	1107	208	0.2	0.7	12	0.47
− 2445	254	1149	23	248	7.4	12.0	− 21	4.39
− 1476	403	916	615	207	4.7	7.2	61	1.07
− 383	444	222	1840	186	0.5	1.4	199	2.72
− 827	82	548	2406	204	2.7	4.2	− 41	0.78
− 401	218	114	940	197	0.3	1.8	23	3.25
− 316	361	197	1966	185	0.5	1.3	20	1.26
− 2138	446	1231	12	213	6.9	10.0	− 15	3.07
− 809	158	312	870	231	1.4	3.8	1	1.98
− 1031	129	560	553	211	2.8	5.2	− 30	0.77
− 1803	523	854	19	218	4.4	8.5	50	5.55
− 466	271	351	1736	192	1.4	2.2	− 1	0.79
− 1308	168	590	56	228	3.1	6.5	− 33	2.78
− 583	134	293	1704	193	1.4	2.8	− 8	1.03
− 1142	540	544	38	203	2.1	5.1	108	5.03
− 672	315	527	2315	191	2.3	3.2	55	0.82

Table 5. Checking exemplars: sensors measurements, and *DD* and *Ra*

F_x (N)	F_r (N)	F_z (N)	*Vb* (mv)	*AE* (mv)	D_z (μm)	D_x (μm)	*DD* (μm)	*Ra* (μm)
− 231	124	123	1871	192	0.5	1.1	2	0.82
− 453	179	140	2407	176	0.6	2.1	20	2.40
− 534	99	322	1881	193	1.5	2.8	− 16	0.881
− 398	147	183	2868	191	0.6	1.7	4	.10
− 168	68	112	1683	207	0.5	1.0	− 10	0.90

$$SS_F = \sum_{i=1}^{K_F} \frac{F_i^2}{n_{F_i}} - \frac{T^2}{N} \quad \text{and} \quad SS_T = \sum_{i=1}^{N} y_i^2 - \frac{T^2}{N} \tag{2,3}$$

V_e is the variance due to the error and is given by

$$V_e = \frac{SS_T - \sum_F SS_F}{N - 1 - \sum_F \nu_F} \tag{4}$$

where:

ν_F number of degrees of freedom associated with factor F; $\nu_F = K_F - 1$;

K_F number of levels for factor F;

n_{Fi} number of observations y under level i of factor F;

T sum of all observations;

N total number of observations (e.g. $N = 16$ in Tables 2 and 4);

F_i sum of observations under ith level of factor F.

Another interesting way to analyze the effect of a given factor on sensor responses is to plot the graph of average effects. In this graph, the horizontal and the vertical axes indicate the factor levels and the characteristic magnitude, respectively. The plotted points correspond simply to the averages of all the observations realized under each factor level

(F_i/n_{Fi}). As the experiments were designed using an orthogonal array, the estimates of the average effects will not be biased.

2.2. *Analysis of quality sensitivity to changes in process conditions and cutting parameters*

Fig. 6 shows that *Ra* and *DD* are affected at different degrees by all process conditions and cutting parameters. In particular, *DD* seem to be more sensitive to changes in process conditions and cutting parameters than *Ra*. Wear appeared as the most important uncontrolled factor for *DD*. However, no factor apart from feed rate has a particular effect on *Ra*. Similar conclusions can be clearly established from the percent contributions reported in Table 6.

Fig. 6(a) and (b) shows that the process parameters mostly affecting quality in machining are the cutting feed and the depth of cut. The effects of the cutting speed were negligible. These results are expected since the cutting forces, which are recognized to have a significant effect on part quality, are more sensitive to changes in the feed and the depth of cut than to variations of the cutting speed [see also Fig. 7(a)–(c)]. Unlike *Ra*, the *DD* depend significantly on *d*. Interestingly, the dimensional errors are very large when *d* is low, and they underside slightly the part when *d* is high. In fact, these results can be explained as follows: when *d* is high, the cutting forces are very important [see Fig. 7(a) and (c)] and thus the heat generated is also important. This results in an expansion in part diameter and consequently more material is removed from the workpiece. However, with a lower *d*, the workpiece is subject to more vibrations [see Fig. 7(d)]. On the other hand, the *Ra* and *DD* show an exponential-like behavior as a function of cutting feed. In Table 7, we observe that feed is correlated to *DD* by up to 30% and to *Ra* by 90%. Accordingly, one can presume that *DD* can be controlled using the cutting feed and the depth of cut, while *Ra* can be controlled only with the cutting feed.

Finally, Table 6 shows that the error contributions associated with *Ra* and *DD* are

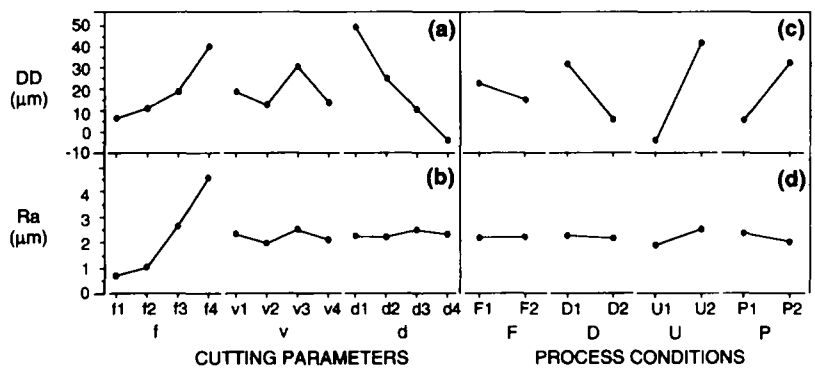

Fig. 6. (a), (b) Effect of process conditions, and (c), (d) effect of cutting parameters on surface finish and dimensional deviations.

Table 6. Percent contributions

	Sensors							Quality characteristics	
	F_t	F_n	F_z	*Vb*	*AE*	D_z	D_t	*DD*	*Ra*
f	27.0	21.9	9.2	47.5	18.4	8.8	23.6	6.0	89.4
v	1.8	0.7	1.0	19.5	2.3	0.2	1.8	0.8	0.3
d	63.2	—	77.3	7.8	21.9	75.1	66.8	12.8	0.3
F	1.2	—	0.2	2.5	8.1	0.3	1.1	0.8	—
D	0.1	0.3	—	—	—	—	—	14.2	—
W	0.6	75.3	4.6	—	19.4	0.3	0.2	42.9	3.1
P	5.4	—	3.0	3.3	2.0	5.4	5.6	14.8	0.8
Error	0.7	1.7	4.7	19.4	27.7	9.9	0.8	7.7	6.0

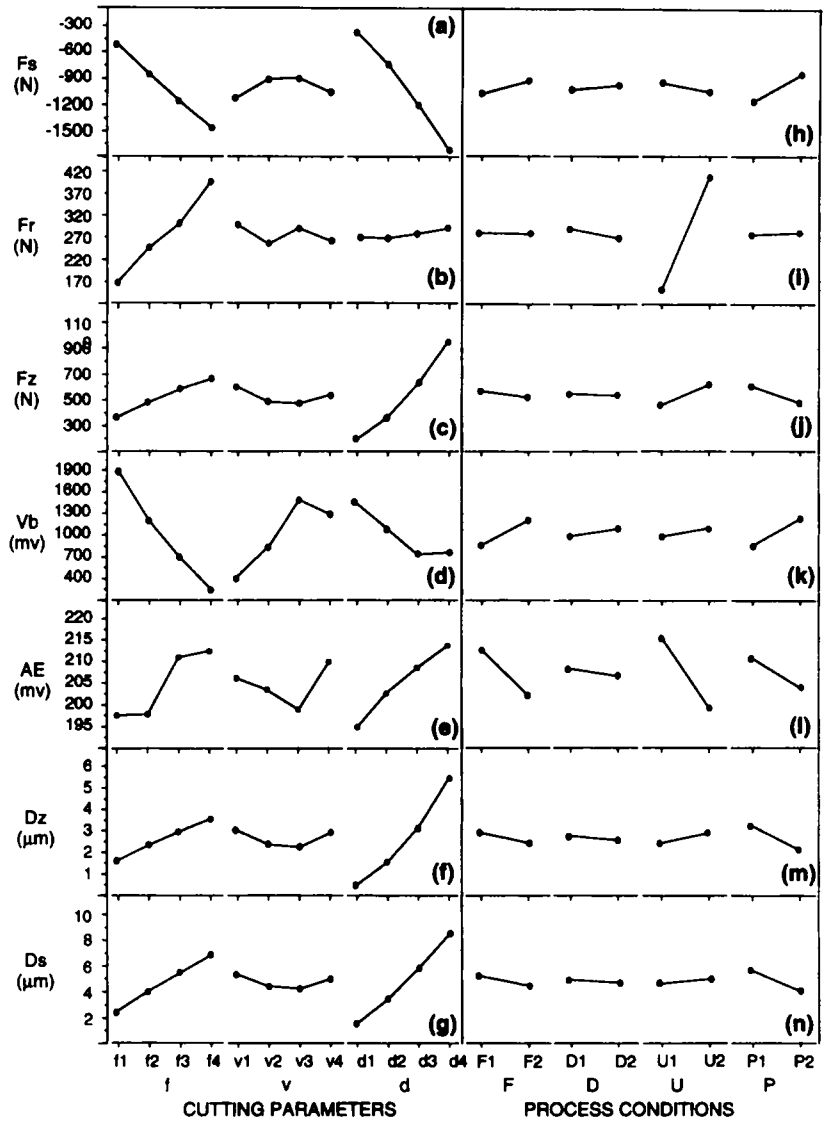

Fig. 7. (a)–(g) Effect of cutting parameters, and (h)–(n) effect of cutting conditions on sensor measurements.

Table 7. Correlations

	DD	*Ra*	$\|DD\| + \|Ra\|$
F_s	0.19	− 0.59	0.78
F_r	0.73	0.61	1.35
F_z	− 0.17	0.43	0.60
Vb	0.05	− 0.68	0.73
AE	− 0.44	0.42	0.86
D_z	− 0.30	0.40	0.70
D_s	− 0.20	0.60	0.80
f	0.30	0.90	1.20
v	0.00	0.00	0.00
d	− 0.40	0.10	0.50

acceptable (less than 8%). This implies that the most important process conditions and cutting parameters that influence these characteristics were included in the experiment.

2.3. *Analysis of sensor responses*

Fig. 7 shows the average effect of process conditions and cutting parameters on sensor outputs as obtained from the data of Tables 2 and 4. Apparently, tool wear has a significant effect on acoustic emissions, while the vibrations are much affected by cutting feed. However, Table 6 shows that the error contribution associated with these two sensors is very high, indicating that other factors could perturb the generated acoustic emissions and vibrations during the cutting operation. Accordingly, the latter two variables cannot be used reliably to monitor *Ra* and *DD* in turning. F_z and D_z have similar responses to all of the process conditions and cutting parameters, while F_s and D_s have also similar but sign different responses. However, as can be seen from Table 6, the force signals are more affected by tool feed and wear, and have lower error contributions than those associated with tool deflection signals. It was shown previously that feed and wear are very important for *Ra* and *DD*, respectively. Interestingly, the normal force shows an excellent sensitivity to tool wear and cutting feed. Furthermore, Table 7 shows that the highest cumulative correlation values are associated with cutting feed and normal force. Thus one can expect to use these latter factors in the fusion model.

Finally, shown in Table 8 are the standard deviations of the sensor signals as calculated using the data obtained from the repetitions of the second set of tests. It can be observed that there is an important variability (16.49%) in the response of the accelerometer. Therefore, this sensor is not as repeatable as the others and should be rejected. On the other hand, the percentage of error of *Ra* and *DD* measurements were as high as 11.40 and 14.73%, respectively. This variability can be attributed to measurement errors, and to the effect of some unknown factors such as variations in the characteristics of the cutting tools.

Even if the sensors could be selected based on the above analysis, it still remains difficult to realize and it is widely affected by the fusion model selected. Thus, a systematic and rigorous procedure for the selection of the best sensors comprising modeling considerations is required for better sensor fusion.

3. SENSOR FUSION

3.1. *The proposed method for sensor selection and fusion*

The basic idea behind the proposed procedure for sensor selection and fusion is to select sensors by minimizing the modeling error on *Ra* and *DD*. It uses the neural network modeling technique which has shown great capabilities to build models without overfitting, despite incomplete or noisy data. Basically, a pre-determined number of neural networks are trained. Each network is designed with a different set of input sensors selected based on an orthogonal array (OA). On selecting the OA to design the networks to be trained, each sensor is considered as one parameter with two levels: present (*P*1) or not (*P*0) among the set of the inputs. Thus, the average effect of every sensor on the performance criterion can be computed as follows:

$$\text{Effect of } P = (\text{Average performance at level } \text{"}P1\text{"} \text{ of parameter } P) - (\text{Average performance at level } \text{"}P0\text{"} \text{ of parameter } P) \quad (5)$$

Table 8. Standard deviations

	Standard deviations	Typical values	Error (%)
F_s	5.4568	− 996.60	0.75
F_r	5.0858	284.24	1.78
F_z	4.1892	529.97	0.79
Vb	167.0534	1012.65	16.49
EA	8.1075	207.45	3.91
D_z	0.0553	2.6313	2.10
D_s	0.0819	4.74	1.73
DD	2.7899	18.94	14.73
Ra	0.2549	2.24	11.40

The performance criterion of the sensing system can be defined by a measure of the sum of squared error SE_T, between the sensing system estimates $E_{i,j}$, and the desired output $D_{i,j}$, summed over all model outputs. This is given by;

$$SE_T = \frac{1}{2} \sum_i \sum_j (E_{i,j} - D_{i,j})^2 \tag{6}$$

where i indicates the ith tested I–O exemplar (i.e. a line of data from Tables 2 and 4) and j is the jth neural net output estimated from the same ith input exemplar. In addition to the data set required for training, it is recommended to use a second data set to check the network accuracy, overfitting and generalization. Thus SE_T becomes:

$$SE_T = SE^t + SE^c \tag{7}$$

where SE^t and SE^c are the sums of the squared errors obtained from the training and the checking data sets, respectively.

Finally, only the sensors that improve the performance of the sensing system are selected, otherwise they are discarded. The final fusion model is established by training a new neural network.

3.1.1. *Introduction to neural networks.* As shown in Fig. 8, a neural network consists of N neurons, each of which is connected to the neurons of the adjacent layers. A threshold value θ_j is associated with each neuron. The output of each neuron is determined by the level of the input signal in relation to the threshold value. These signals are modified by the connection weights (also called synaptic strengths) between the neurons.

We implement the sigmoidal function to compute the output of a given neuron. Let O_j be the output of the current neuron, O_i the output of neuron i of the preceding layer and W_{ij} the weight of the connection between the two neurons. Then the input to the jth node is given by:

$$I_j = \sum_i W_{ij} O_i + \theta_j \tag{8}$$

The multilayered perceptron networks will be trained using the quasi-Newton procedure [20, 21]. This procedure is basically an optimization technique designed to minimize E, the sum of the squared errors between the estimated network outputs S_{pj} and the desired outputs Y_{pj} over the N exemplars in the training data set, each of them containing M outputs:

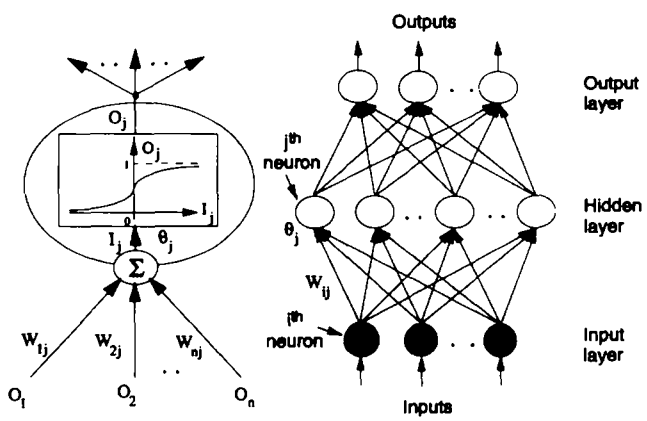

Fig. 8. Multilayered feed forward network.

$$E = 0.5 \sum_{p=1}^{N} \sum_{j=1}^{M} (S_{pj} - Y_{pj})^2 \tag{9}$$

The initial weights and thresholds are usually set to small random values. The exemplar values input in the neural network are linearly mapped to a 0–1 range. The neural net outputs will allow values between 0 and 1 which can be mapped back to full range.

3.2. *Application*

In addition to process input parameters and sensor information, Fig. 9 shows that the network configuration is also considered as a parameter for the design of the fusion models to be tested. This parameter was assigned three levels. Each level indicates a different configuration of the network hidden layer which are $Z \times 5 \times 2$, $Z \times 3 \times 2$ and $Z \times 5 \times 3 \times 2$, respectively, Z being the number of inputs as shown in Tables 9–11. In Table 9, the (i) and (—) indicate, respectively, whether the information at the top of the column is input to the fusion model or not. In the first ten models (models 1–10), only one input is utilized and the network configuration remains $1 \times 3 \times 2$, while models 11 through 26 were designed using an orthogonal array. The orthogonal array that best suits our problem is the L_{16}.

The training data set is provided in Tables 2 and 4. A total of 16 exemplars were used for training purposes. The checking data were the same as those formed in studying sensor repeatability. All six repetitions were considered resulting in 30 checking exemplars. Tables 3 and 5 shows the 5th repetition. Notice that the parameters of the first three checking tests were set using conditions chosen inside the training region of Tables 2 and 4, while the cutting speed of the fourth test and the feed rate of the fifth test have been set near but outside the trained region. The process conditions (F, D, W and P) were set to intermediate levels with respect to those used during training.

The accuracy of the designed models is presented in Table 10 where the squared errors as obtained from the training and the checking data for every single network output (SE_{Ra}^t, SE_{DD}^t, SE_{Ra}^c, and SE_{DD}^c) and the number of training epochs are reported. Also shown in Table 10 is the total squared error ($SE_T = SE^c + SE^c = SE_{Ra}^t + SE_{DD}^t + SE_{Ra}^c + SE_{DD}^c$). For the sake of comparison, all the squared errors were calculated using normalized network outputs.

In models 1 through 10 where only one sensor is used, the network was incapable of modeling with accuracy the *DD* and *Ra* characteristics. The most acceptable results were obtained from the feed and the radial force (see Table 10). However, no sensor can be discarded at this stage. In fact, a sensor with a relatively high squared error may significantly reduce the errors if it happens to be the only one correlated to a specific mechanism influencing the *DD* and *Ra*. Using the data obtained from the results of models 11 through 26 planned according to the OA, the average effect of each sensor's information and the network configuration on the sensing system performance SE_T was calculated. The average

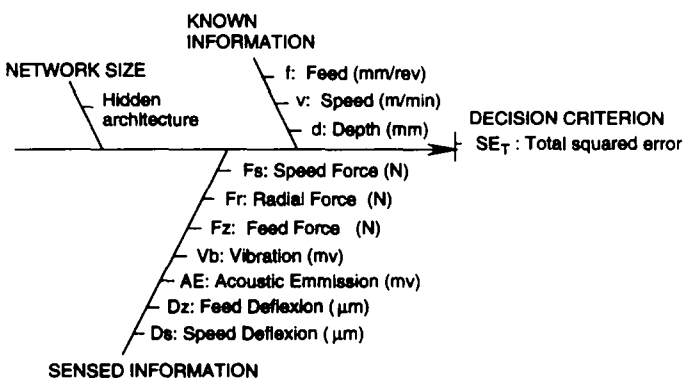

Fig. 9. Inputs and network size selection.

Table 9. The designed models

Model number	Inputs (cutting parameters and sensors)										Network architecture
	f	v	d	F_x	F_r	F_z	Vb	AE	D_z	D_x	
1	i	—	—	—	—	—	—	—	—	—	× 3 × 2
2	—	i	—	—	—	—	—	—	—	—	× 3 × 2
3	—	—	i	—	—	—	—	—	—	—	× 3 × 2
4	—	—	—	i	—	—	—	—	—	—	× 3 × 2
5	—	—	—	—	i	—	—	—	—	—	× 3 × 2
6	—	—	—	—	—	i	—	—	—	—	× 3 × 2
7	—	—	—	—	—	—	i	—	—	—	× 3 × 2
8	—	—	—	—	—	—	—	i	—	—	× 3 × 2
9	—	—	—	—	—	—	—	—	i	—	× 3 × 2
10	—	—	—	—	—	—	—	—	—	i	× 3 × 2
11	i	i	i	i	i	i	i	i	i	i	× 5 × 2
12	i	i	i	i	i	i	—	—	—	—	× 5 × 2
13	i	i	—	—	—	—	i	i	i	i	× 5 × 2
14	i	i	—	—	—	—	—	—	—	—	× 5 × 2
15	—	—	i	i	—	—	i	i	—	—	× 5 × 2
16	—	—	i	i	—	—	—	—	i	i	× 5 × 2
17	—	—	—	—	i	i	i	i	—	—	× 5 × 2
18	—	—	—	—	i	i	—	—	i	i	× 5 × 2
19	i	—	i	—	i	—	i	—	i	—	× 3 × 2
20	i	—	i	—	i	—	—	i	—	i	× 5 × 3 × 2
21	i	—	—	i	—	i	i	—	i	—	× 5 × 3 × 2
22	i	—	—	i	—	i	—	i	—	i	× 3 × 2
23	—	i	i	—	—	i	i	—	—	i	× 5 × 3 × 2
24	—	i	i	—	—	i	—	i	i	—	× 3 × 2
25	—	i	—	i	i	—	i	—	—	i	× 3 × 2
26	—	i	—	i	i	—	—	i	i	—	× 5 × 3 × 2
27	i	—	i	—	i	i	—	—	—	—	× 3 × 2
28	i	—	—	—	i	i	—	—	—	—	× 3 × 2
29	—	—	—	—	i	i	—	—	—	—	× 3 × 2
30	i	—	i	—	i	—	—	—	—	—	× 3 × 2

i, Parameter or sensor is considered as an input; —, not considered.

effect graph is depicted in Fig. 10. This graph shows that the only sensor signals that could significantly reduce the SE_T are the cutting feed, the depth of cut, and the radial and z-axis forces. The best network configuration is the $4 \times 3 \times 2$ with three neurons in the hidden layer.

Accordingly, model 27, also shown in Fig. 11, was built using the sensors and network configuration selected above (f, d, F_r, F_z and $4 \times 3 \times 2$). Effectively, Table 10 shows that this model performs better than all former ones. Also, the learning speed was much improved.

In Fig. 12, the experimental measurements used for the checking exemplars are compared to corresponding model 27 estimates. Globally, the performance of the fusion model was excellent. The small differences that can be observed may be attributed to many factors. In fact, *Ra* is affected by many complex mechanisms that may arise during the machining process. For instance, at relatively high speeds, chatter is the main source of roughness, while at low speeds, built-up edge may be dominant. On the other hand, the *DD* depend greatly on the measuring procedure and on the experimenter himself. Their small values are probably the main factor for the significant experimental errors. The effect of tool wear was very dominant and could have slightly biased the results. Finally, it was noticed that few exemplars were used to build the fusion model and that only two and four levels were considered for the cutting conditions and the cutting parameters, respectively. One can conclude that the OA test strategy is a relevant approach for obtaining a complete design, and that neural networks are able to extract the required information from limited data. Finally, it must be remembered that the experimental data used throughout this study has its own level of inaccuracy.

To check the performance of the selection procedure, models 28, 29 and 30 were trained

Table 10. Precisions of models

Model number	$SE_{DD}^{\wedge}$	$SE_{Ra}^{\wedge}$	$SE_{DD}^{\vee}$	$SE_{Ra}^{\vee}$	SE_T	Epochs
1	0.508	0.057	0.079	0.326	0.970	139
2	0.535	0.621	0.211	0.571	1.939	168
3	0.469	0.621	0.540	0.536	2.168	276
4	0.969	0.355	0.266	0.278	1.379	623
5	0.105	0.259	0.181	0.204	0.751	561
6	0.311	0.444	0.721	0.398	1.875	450
7	0.381	0.174	0.265	0.182	1.003	1660
8	0.339	0.326	0.861	1.283	2.810	1044
9	0.213	0.277	0.352	0.208	1.050	367
10	0.370	0.322	0.362	0.720	1.780	1500
11	0.0	0.0	0.503	0.692	1.195	379
12	0.0	0.0	0.083	0.105	0.188	739
13	0.0	0.0	3.107	1.126	4.376	444
14	0.004	0.021	0.483	0.155	0.946	2294
15	0.199	0.007	1.490	1.605	3.302	3226
16	0.006	0.007	0.475	0.087	0.898	3469
17	0.001	0.001	1.165	0.600	1.766	1200
18	0.001	0.001	2.177	0.255	2.433	1688
19	0.003	0.007	0.362	0.245	0.617	749
20	0.001	0.004	0.832	0.176	1.014	8000
21	0.007	0.0	1.015	0.470	1.493	1062
22	0.002	0.005	1.012	0.855	1.876	2183
23	0.007	0.022	0.924	0.531	1.485	1682
24	0.002	0.014	0.832	0.532	1.380	1594
25	0.019	0.056	2.822	0.482	3.380	1672
26	0.090	0.086	3.139	0.476	3.792	817
27	0.004	0.006	0.017	0.077	0.103	209
28	0.005	0.006	0.021	0.100	0.133	266
29	0.091	0.111	0.063	0.163	0.429	779
30	0.031	0.013	0.231	0.114	0.389	768

Table 11. Correlation

Model number	r_{DD}^2	r_{RA}^2
1	0.1746	0.7846
2	0.1307	0.2023
3	0.3186	0.1792
4	0.2252	0.3786
5	0.7385	0.5177
6	0.4453	0.3113
7	0.3358	0.6897
8	0.4812	0.4585
9	0.5570	0.5244
10	0.3753	0.5464
11	0.7447	0.7369
12	0.8739	0.9078
13	0.5987	0.6315
14	0.5723	0.8427
15	0.5698	0.6621
16	0.6641	0.9219
17	0.6203	0.7103
18	0.5291	0.8287
19	0.6878	0.8369
20	0.5856	0.8371
21	0.7169	0.9291
22	0.5776	0.7053
23	0.5527	0.7167
24	0.6319	0.6977
25	0.6257	0.6807
26	0.6174	0.4587
27	0.9695	0.9270
28	0.9612	0.9124
29	0.7762	0.8613
30	0.7254	0.8984

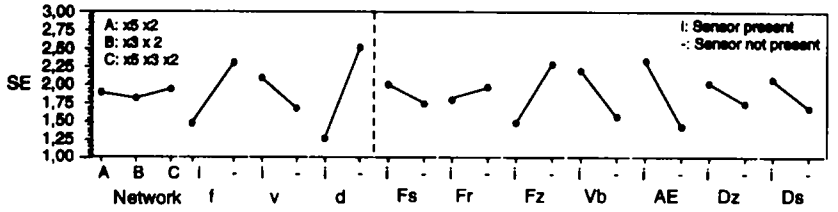

Fig. 10. Average effect of sensors and network size on the sensing system performance (SE_T).

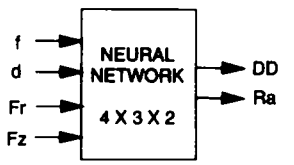

Fig. 11. The final model.

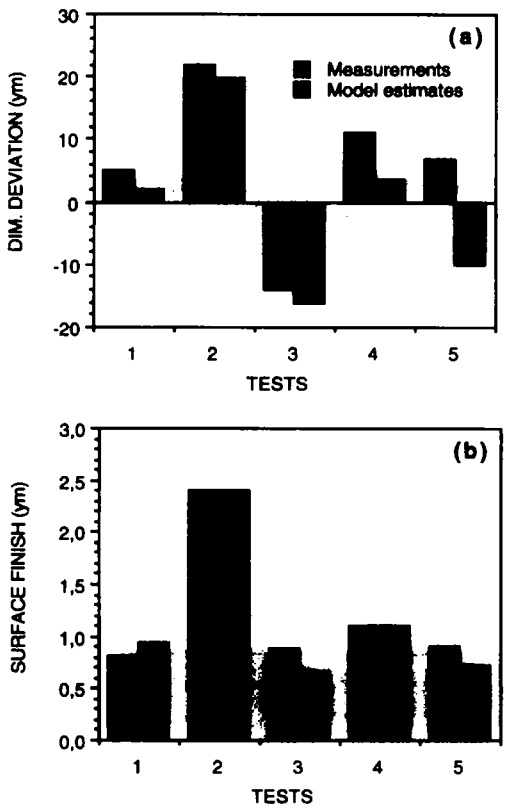

Fig. 12. A comparison between experimental measurements used for the checking exemplars and the corresponding model 27 estimates.

with the feed, depth of cut and the z-axis force omitted, respectively. No improvement was observed. As it can be seen in Table 10, the results were very poor. Specifically, when the feed or force in feed direction were omitted as in models 29 and 30, respectively, the prediction errors become very high.

The analysis of correlation is another interesting tool that can be used to study the statistical relationships between the outputs of the models and the experimental data. Let Y_i and Y_i^c represent a measured variable and a modeled variable, respectively. Then, the coefficient of correlation r^2 between these two variables can be evaluated as follows:

$$r^2 = \frac{\sum_i (Y_i^c - \bar{Y})^2}{\sum_i (Y_i^c - \bar{Y})^2 + \sum_i (Y_i - \bar{Y})^2} \tag{10}$$

where $\bar{Y}$ is the average value of variable Y. Table 11 shows the coefficients of correlation observed between the measured surface finishes and dimensional deviations (from the training and the checking data sets) and the corresponding output from each of the 30 trained models. This table shows in general that the majority of the trained models could not explain satisfactorily the variations of the measured values. The best results can only be observed with the models that include much of model 27's inputs among their own set of inputs (see the results obtained from models 1, 2 or 28). As it was expected, model 27 provided the best correlation with the experimental data. Interestingly, this result was obtained with the two outputs of the network.

To confirm the advantage of the neural network modeling technique over theoretical models, we compared the surface finish obtained experimentally with predicted values determined using the neural model 27 and a commonly used theoretical model from Boothroyd [22] and given by:

$$Ra = \frac{0.0321\, f^2}{r_e} \tag{11}$$

where r_e is the tool corner radius (in mm). The comparative results shown in Table 12 indicate that the neural model presented an average and maximum error at least six times lower than the theoretical model.

According to the authors, the model obtained from the proposed sensor fusion method can be reliably used for on-line control and monitoring of the turning process on free-machining and low carbon steels.

4. DISCUSSION AND TRENDS

In the course of this study, the response of several basic sensors was analyzed, and their correlation with *Ra* and *DD* during the cutting operation was also investigated under several practical process conditions. On the other hand, the proposed sensor fusion method successfully selected the sensors whose signals carry the best information about the state of the machining operation. The cutting feed, the depth of cut, and the radial and z-axis cutting forces were found to comprise the only information that is needed. Using this

Table 12. Comparison to theoretical surface finish

	Exemplar number	Measured *Ra* (μm)	Neural model 27 (μm)	Theoretical model (μm)
Training exemplars (Tables 2 and 4)	1	0.47	0.92	0.40
	2	4.39	4.45	6.47
	3	1.07	1.25	1.61
	4	2.72	2.66	3.64
	5	0.78	0.51	0.40
	6	3.25	3.32	6.47
	7	1.26	1.40	1.61
	8	3.07	3.01	3.64
	9	1.98	1.81	3.64
	10	0.77	0.68	1.61
	11	5.55	5.48	6.47
	12	0.79	0.72	0.40
	13	2.78	2.84	3.64
	14	1.03	0.92	1.61
	15	5.03	5.00	6.47
	16	0.82	0.70	0.40
Tables 3 and 5	1	0.82	0.94	0.63
	2	2.40	2.40	4.95
	3	0.88	0.66	0.63
	4	1.10	1.10	1.61
	5	0.90	0.73	0.10
Average error		—	0.12	0.93
Maximum error		—	0.45	3.22

information, the fusion model was established by training a neural network with only three hidden neurons using 16 exemplars obtained under a variety of machining conditions and parameters. The results are very promising. The surface finish was assessed with an error varying from 2 to 25% under different cutting conditions and parameters, while dimensional deviations varying from -20 to $+20$ μm were predicted with an average error of 6 μm. Finally, this paper also demonstrated the performance of neural networks in situations where nonlinear mappings must be automatically acquired from the training data. The governing relationships were extracted from experimental data in which a high level of noise may be present.

In future work, machining experiments will be run in order to test the developed sensing system within an intelligent control scheme. The sensing system must feed the controller with on-line estimates of the *Ra* and *DD* of the machined part. Based on these estimates, the controller will adjust the cutting parameters in order to optimize quality, accommodate the variations of the process conditions and improve productivity.

Acknowledgements—The authors are grateful to Natural Sciences and Engineering Research Council of Canada (grant number OPG0089759) for their financial assistance to the project.

REFERENCES

[1] Dickinson, G. R., Survey of factors affecting surface finish. *Proc. Instn Mech. Engrs*, 1967, **182**, 135.
[2] Ulsoy, A. G., Koren, Y. and Rasmussen, F., Principal developments in the adaptive control of machine tools. *ASME J. Dyn., Syst. Meas. Control*, 1983, **105**, 107.
[3] Ulsoy, A. G. and Koren, Y., Applications of adaptive control to machine tool process control. *IEEE Control Syst. Mag.*, 1989, **9**, 33.
[4] Watanabe, T. and Iwai, S., A control system to improve the accuracy of finished surfaces in milling. *Trans. ASME*, 1983, **105**, 192.
[5] Tlusty, J. and Andrews, G. C., A critical review of sensors for unmanned machining. *Ann. CIRP*, 1983, **32**, 563.
[6] Dornfeld, D. A., Monitoring the machining process by means of acoustic emission sensors. In *Acoustic Emission: Current Practice and Future Directions* (edited by W. Sachse, J. Roget and K. Yamaguchi) ASTM STP 1077. American Society for Testing and Materials, Philadelphia, PA, 1991.
[7] Lundholm, T., Yngen, M. and Lindstrom, B., Advanced process monitoring—a major step towards adaptive control. *Robot. Comput.—Integrat. Manufact.*, 1988, **4**, 413.
[8] Birla, S. K., Sensors for adaptive control and machine diagnostics, *Proc. Machine Tool Task Force Conf.*, 1980, **4**, Section 7–12.
[9] El-Karamany, Y., Turning long workpieces by changing the machining parameters. *Int. J. Mach. Tool Des. Res.*, 1984, **24**, 1.
[10] Luk, F., Huynh, V. and North, W., Application of spatial spectral analysis to inline machining inspection of surface roughness. In *Recent Developments in Production Research*, p. 59. Elsevier, Amsterdam, 1988.
[11] Dornfeld, D. A., Sensor Fusion. In *Handbook of Intelligent Sensors for Industrial Automation* (edited by N. Zueck). Addison-Wesley, Reading, MA, 1991.
[12] Guillot, M., Azouzi, R. and Coté, M. C., Process monitoring and control. In *Artificial Neural Networks for Intelligent Manufacturing* (edited by C. Dagli). Chapman and Hall, London, 1994.
[13] Rangwala S. and Dornfeld, D., Integration of sensors via neural networks for detection of tool wear states. In *Intelligent and Integrated Manufacturing Analysis and Synthesis* (edited by C. R. Liu *et al.*), Winter Annual Meeting ASME, Boston, MA, 1987.
[14] Chryssolouris, G. and Guillot, M., A comparison of statistical and AI approaches to the selection of process parameters in intelligent machining. *Trans. ASME, J. Engng Ind.*, 1990, **112**, 122.
[15] Lippmann, R. P., An introduction to computing with neural nets. *IEEE ASSP Mag.*, 1987, April, 4.
[16] Simpson, P. K., Foundations of neural networks. *Artificial Neural Network, Paradigms, Application and Hardware Implementations*. IEEE Press, 1992.
[17] Box, G. E. P., Hunter, W. G. and Hunter, J. S., *Statistics for Experimenters: An Introduction to Design, Data Analysis and Model Building*. Wiley, New York, 1978.
[18] Taguchi, G., Elsayed, E. A. and Hsiang, T., *Quality Engineering Product and Process Design Optimization*. McGraw-Hill, New York, 1986.
[19] Ross, P. J., *Taguchi Techniques for Quality Engineering*. McGraw-Hill, New York, 1988.
[20] Gil, P., Murray, W. and Wright, M., *Practical Optimization*. Academic, New York, 1981.
[21] Watrous, R. L., Learning algorithms for connectionist networks: applied gradient methods of nonlinear optimization. *1st IEEE Int. Conf. on Neural Networks*, 1987, **2**, pp. II.619–II.627.
[22] Boothroyd, G., *Fundamental sof Metal Machining and Machine Tools*. Dekker, New York, 1989.